Comparison of (5+2) Cycloadditions Involving Oxidopyrilium and Oxidopyridinium Ions – Relative Reactivities

Yining Lu and Dean J. Tantillo*

Department of Chemistry, University of California, Davis, CA 95616

** djtantillo@ucdavis.edu*

Abstract

A variety of (5+2) cycloaddition reactions involving oxidopyridinium and oxidopyrilium zwitterions are compared to investigate the effects of nitrogen-for-oxygen substitution on reactivity. Activation barriers for nitrogen-containing systems are predicted to be larger than those for analogous oxygen-containing systems. Correlations between barrier heights and synchronicity of C–C bond formation, changes to aromaticity, reactant distortion, and interaction energies between zwitterions and alkenes were assessed, leading to the conclusion that reactivity depends more on distortion effects (including aromaticity loss) than on interaction effects (such as those associated with HOMO-LUMO interactions).

Introduction

The synthesis of many complex organic molecules has benefited from the development of cycloadditions between oxidopyrilium zwitterions and alkenes.[1,2,3] Analogous (5+2) cycloadditions involving oxidopyridinium zwitterions also have been used to advantage.[2,3] Figure 1 shows four such examples from elegant natural product syntheses.[4-7] Here we explore the effects of exchanging oxidopyrilium O atoms for oxidopryridium NR groups using computational methods. Previously, the reactivities of benzene and tetrazines in [4+2] cycloadditions were compared, and it was found that nitrogen substitution increases reactivity.[8-11] The increased reactivity was attributed to a decrease in aromaticity, i.e., disruption of aromaticity was associated with a smaller

energetic penalty.[8] Changing a pyrilium O for an NR group has been found to change the reactivity of these ylides,[9-11] and we hypothesized that changes to the aromaticity of the ring may be responsible for these differences; the effects of this change on barriers for (5+2) cycloadditions were thus explored here using density functional theory (DFT) calculations.

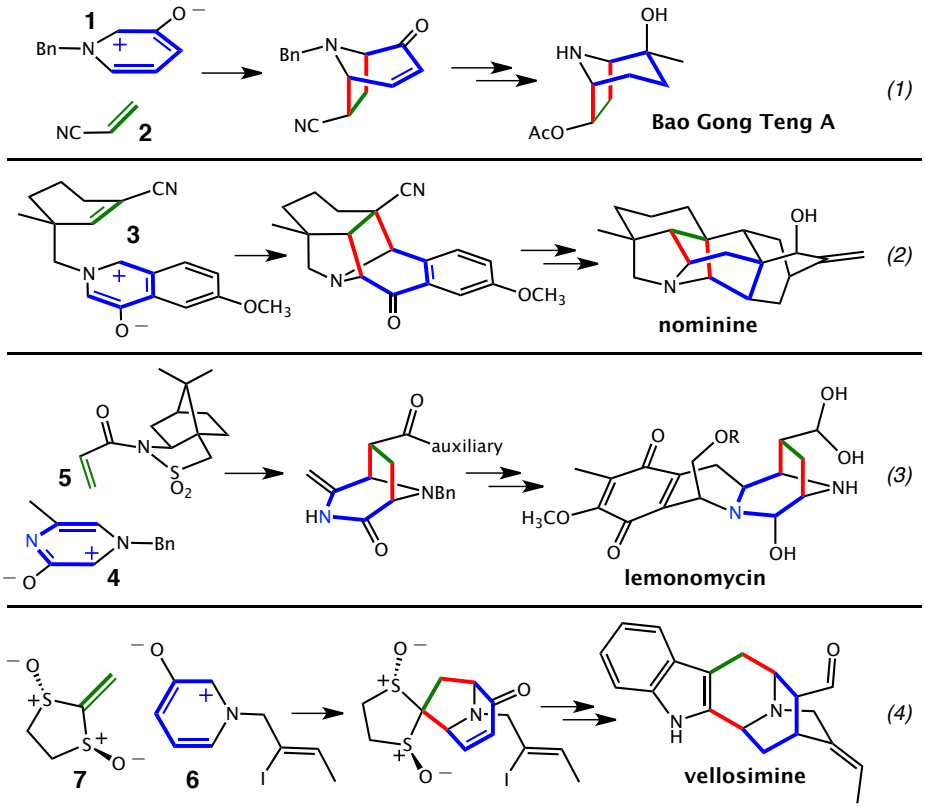

Figure 1. Synthetically useful (5+2) cycloadditions of oxidopyridinium zwitterions (or closely relates structures; reactions *2* and *3*). Resonance structures highlighting the cationic, 4-electron, 5-atom substructure are highlighted in blue. The two atoms in the alkene are highlighted in green. The two C–C σ-bonds formed in the cycloaddition are highlighted in red.

In analogy to previous work,[15] we used the alkenes shown at the top of Figure 2, here paired with the ions shown at the bottom of Figure 2. In addition, we examined the cycloadditions shown in Figure 1. Computed activation barriers, transition state structure (TSS) geometries, HOMO/LUMO energies, nucleus independent chemical shift (NICS) values,[16] and endo/exo selectivities are compared to assess the effects of

nitrogen substitution.

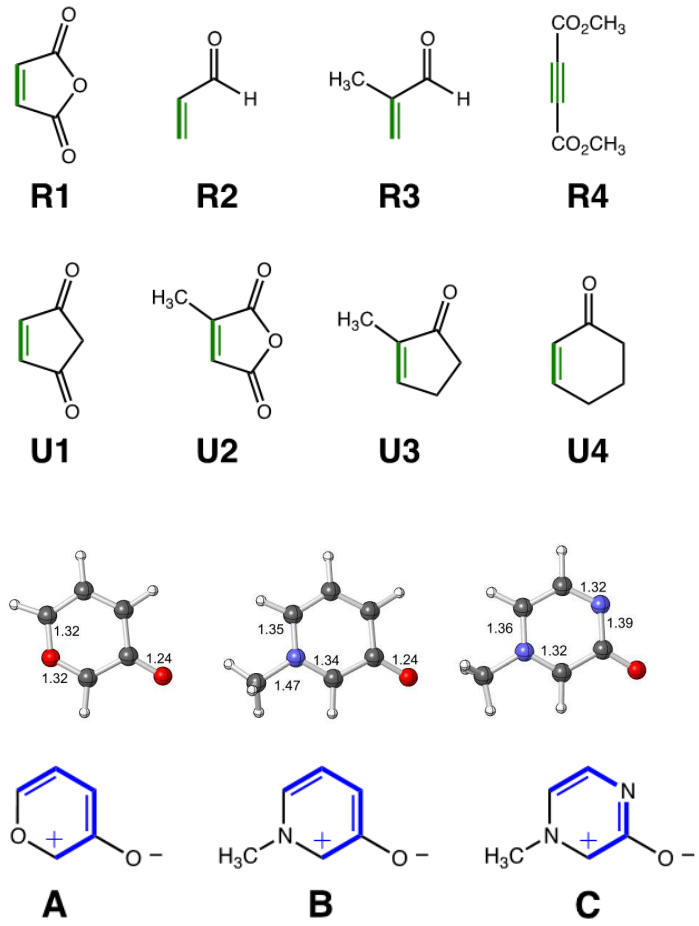

Figure 2. Cycloaddition partners. **R** labels indicate the four most reactive alkenes; **U** labels indicate the four least reactive alkenes. Selected distances (Å; M06-2X/6-31+G(d,p)) are shown for zwitterions **A**-**C**.

COMPUTATIONAL METHODS

All computations were carried out using Gaussian 09.[17] Optimizations were performed at three different levels: B3LYP[18]/6-31+G(d,p), B3LYP-D3[19]/6-31+G(d,p), and M06-2X[20]/6-31+G(d,p) (except for **E**, for which only M06-2X[20]/6-31+G(d,p) was used; see below). All stationary points were characterized as either minima or TSSs based on frequency analysis. IRC calculations[21] were carried out to confirm the identities of TSSs. For the cycloaddition between **U3** and **B** at the B3LYP[10]/6-31+G(d,p) level, IRC calculations proved problematic, so the TSS was distorted along the reaction coordinate (corresponding to the imaginary frequency) and optimizations were performed on the

distorted structures to find minima. Zwitterions are named with letters **A**-**C**. Prime symbols are used to indicate regiochemistry, with prime labels indicating that the sterically bulkier end of the alkene was proximal to the C–O^- substructure of the zwitterion. Alkenes are named with **Rn** or **Un** labels, depending on whether they fall into the more or less reactive half of alkenes examined (see Figure 2). $\Delta E^{\ddagger}$ and $\Delta G^{\ddagger}$ values were computed using separate reactants. $\Delta G^{\ddagger}$ values include standard thermochemical corrections at 298K (the default approach in Gaussian 09).

Results and Discussion

Barriers. Barriers (both $\Delta E^{\ddagger}$ and $\Delta G^{\ddagger}$) computed with M06-2X/6-31+G(d,p) are listed in Tables 1-6; results from B3LYP and B3LYP-D3 calculations can be found in Tables S9-14. In general, predicted barriers decrease on going from B3LYP to B3LYP-D3 to M06-2X, as expected for these levels of theory (see SI).[22,23] In particular, while B3LYP has been used to capture many important features of cycloaddition reactions (including activation barriers for many reactions),[24-27] it is not suited for predicting contributions from dispersion and is known to have difficulty in predicting the relative energies of cyclic and acyclic isomers (likely a dispersion-related problem).[28-30] Nonetheless, all three levels of theory agree as to the relative reactivity of different systems, regioselectivity and endo/exo stereoselectivity. Predicted barriers for N-containing systems **B** and **C** (Table 1-4) are consistently larger than those for oxidopyrilium zwitterion **A** (Table 5).

Table 1. Computed barriers for B + more reactive alkenes/alkyne from Figure 2 (M06-2X/6-31+G(d,p), kcal/mol).

Transition State	$\Delta E^{\ddagger}$	$\Delta G^{\ddagger}$
B-R1-endo	5.5	20.3
B-R1-exo	1.8	16.6
B-R2-endo	6.8	21.8
B'-R2-endo	9.8	24.8
B-R2-exo	6.2	21.1
B'-R2-exo	9.4	24.2
B-R3-endo	10.4	25.3
B'-R3-endo	13.5	28.7
B-R3-exo	4.4	20.1
B'-R3-exo	10.1	25.6
B-R4	2.0	17.3

Table 2. Computed barriers for B + less reactive alkenes from Figure 2 (M06-2X/6-31+G(d,p), kcal/mol).

Transition State	$\triangle E^{\ddagger}$	$\triangle G^{\ddagger}$
B-U1-endo	7.6	22.9
B-U1-exo	7.4	22.4
B-U2-endo	10.5	26.5
B'-U2-endo	10.3	26.3
B-U2-exo	5.9	21.6
B'-U2-exo	5.2	21.1
B-U3-endo	13.6	30.1
B'-U3-endo	18.6	34.7
B-U3-exo	14.9	30.9
B'-U3-exo	17.3	33.5
B-U4-endo	11.5	27.3
B'-U4-endo	16.6	31.5
B-U4-exo	14.0	30.0
B'-U4-exo	17.2	32.5

Table 3. Computed barriers for C + more reactive alkenes/alkyne from Figure 2 (M06-2X/6-31+G(d,p), kcal/mol).

Transition State	$\triangle E^{\ddagger}$	$\triangle G^{\ddagger}$
C-R1-endo	6.6	20.9
C-R1-exo	0.6	15.0
C-R2-endo	5.3	20.1
C'-R2-endo	7.9	22.8
C-R2-exo	4.5	19.1
C'-R2-exo	7.4	22.1
C-R3-endo	8.1	22.9
C'-R3-endo	11.5	26.6
C-R3-exo	1.8	17.4
C'-R3-exo	8.0	23.2
C-R4	2.2	17.0

Table 4. Computed barriers for C + less reactive alkenes from Figure 2 (M06-2X/6-31+G(d,p), kcal/mol).

Transition State	$\triangle E^{\ddagger}$	$\triangle G^{\ddagger}$
C-U1-endo	6.0	21.2
C-U1-exo	5.8	20.7
C-U2-endo	11.1	26.6
C'-U2-endo	11.2	26.8
C-U2-exo	3.8	19.4
C'-U2-exo	3.4	19.3
C-U3-endo	10.4	26.7
C'-U3-endo	15.6	31.8
C-U3-exo	11.3	27.3
C'-U3-exo	14.6	30.7
C-U4-endo	7.6	23.6
C'-U4-endo	12.9	28.1
C-U4-exo	12.0	27.9
C'-U4-exo	14.4	29.5

Table 5. Computed barriers for A + alkenes/alkyne from Figure 2 (M06-2X/6-31+G(d,p), kcal/mol).

Transition State	$\triangle E^{\ddagger}$	$\triangle G^{\ddagger}$	Transition State	$\triangle E^{\ddagger}$	$\triangle G^{\ddagger}$
A-R1-endo	1.1	13.8	**A-U1-endo**	1.4	15.6
A-R1-exo	-2.3	11.4	**A-U1-exo**	-0.6	13.5
A-R2-endo	0.2	14.2	**A-U2-endo**	2.2	17.1
A'-R2-endo	3.3	17.2	**A'-U2-endo**	2.9	17.9
A-R2-exo	-0.3	13.7	**A-U2-exo**	-0.2	14.6
A'-R2-exo	2.7	16.6	**A'-U2-exo**	-0.8	14.5
A-R3-endo	1.0	15.2	**A-U3-endo**	2.4	17.9
A'-R3-endo	4.6	19.0	**A'-U3-endo**	6.8	22.4
A-R3-exo	0.8	15.0	**A-U3-exo**	2.1	17.2
A'-R3-exo	2.5	17.0	**A'-U3-exo**	4.9	20.2
A-R4	-2.3	12.7	**A-U4-endo**	2.2	17.3
			A'-U4-endo	6.8	21.4
			A-U4-exo	2.4	16.8
			A'-U4-exo	6.1	20.5

Table 6. Computed barriers for reactions from Figure 1 (M06-2X/6-31+G(d,p), kcal/mol).

Transition State	$\triangle E^{\ddagger}$	$\triangle G^{\ddagger}$
1-2-endo	7.7	22.6
1'-2-endo	10.8	25.7
1-2-exo	5.1	20.2
1'-2-exo	7.3	22.4
3	24.2	26.4
4-5-endo	0.2	16.4
4'-5-endo	4.1	20.3
4-5-exo	2.7	18.4
4'-5-exo	5.9	21.8
6-7	3.3	18.9
6'-7	5.7	22.0

Frontier orbitals. For all of the cycloadditions examined, the alkene is electron deficient. Consequently, the HOMOs for the zwitterions are involved in the strongest frontier orbital interactions between cycloaddition partners.[31] HOMOs for zwitterions **A**-**C** are shown in Figure 3 and orbital energies are shown in Table 7. While the shape of the HOMO does not change significantly upon O→NR substitution, HOMO energies are predicted to be slightly higher for the N-containing systems, consistent with the relative electronegativities of O and N. In that N-containing zwitterions are predicted to have higher cycloaddition barriers (*vide supra*), this observation indicates that simple frontier orbital arguments are not sufficient to predict relative reactivity in these cases.

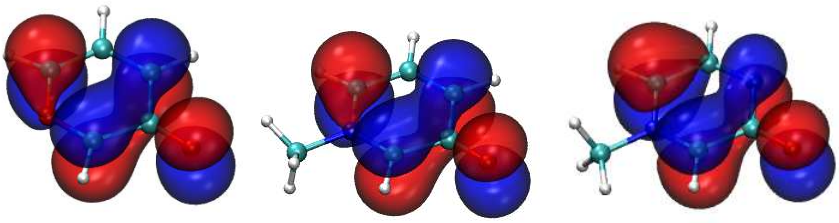

A **B** **C**

Figure 3. HOMOs (M06-2X/6-31+G(d,p)) for **A**-**C**.

Table 7. Frontier orbital Energies for A-C (M06-2X/6-31+G(d,p), eV).

molecule	HOMO energy	LUMO energy
A	-7.3	-1.7
B	-6.7	-0.8
C	-7.3	-1.3

Synchronicity. The differences between the lengths of the two forming C–C bonds (C_a–C_b and C_c–C_d as shown in Figure 4; Tables 8-13) tend to increase on changing from B3LYP to B3LYP-D3 to M06-2X. In addition, differences between the lengths of the forming bonds increase on changing the zwitterion from **A** to **B** to **C**, which correlates with the trend in activation barriers. However, tight correlations between bond length differences and predicted barriers are not found for reactions between a given zwitterion and the series of alkenes in Figure 2 (see Supporting Information for correlation plots).

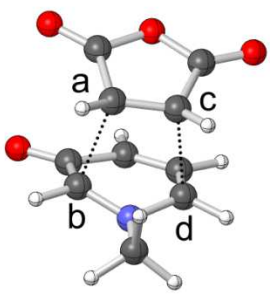

Figure 4. Endo TSS for cycloaddition between **B** and **R1**

Table 8. Distances of forming C–C σ-bonds for reactions involving B and Rn alkenes (M06-2X/6-31+G(d,p)).

Transition State	Ca-Cb (Å)	Cc-Cd (Å)	Difference Between Ca-Cb and Cc-Cd (Å)
B-R1-endo	2.20	2.23	0.03
B-R1-exo	2.08	2.29	0.21
B-R2-endo	2.05	2.41	0.36
B'-R2-endo	2.34	2.12	0.22
B-R2-exo	2.04	2.46	0.42
B'-R2-exo	2.38	2.10	0.28
B-R3-endo	2.01	2.44	0.43
B'-R3-endo	2.38	2.07	0.31
B-R3-exo	1.93	2.86	0.93
B'-R3-exo	2.54	2.00	0.54
B-R4	2.38	2.11	0.27

Table 9. Distances of forming C–C σ-bonds for reactions involving B and Un alkenes (M06-2X/6-31+G(d,p)).

Transition State	Ca-Cb (Å)	Cc-Cd (Å)	Difference Between Ca-Cb and Cc-Cd (Å)
B-U1-endo	2.17	2.21	0.04
B-U1-exo	2.06	2.29	0.23
B-U2-endo	2.19	2.22	0.03
B'-U2-endo	2.18	2.22	0.04
B-U2-exo	1.97	2.42	0.45
B'-U2-exo	2.15	2.16	0.01
B-U3-endo	2.34	2.07	0.27
B'-U3-endo	2.05	2.34	0.29
B-U3-exo	1.88	2.66	0.78
B'-U3-exo	2.50	1.99	0.51
B-U4-endo	2.13	2.23	0.10
B'-U4-endo	2.26	2.13	0.13
B-U4-exo	2.09	2.29	0.20
B'-U4-exo	2.24	2.17	0.07

Table 10. Distances of forming C–C σ-bonds for reactions involving C and Rn alkenes (M06-2X/6-31+G(d,p)),.

Transition State	Ca-Cb (Å)	Cc-Cd (Å)	Difference Between Ca-Cb and Cc-Cd (Å)
C-R1-endo	2.21	2.27	0.06
C-R1-exo	2.05	2.36	0.31
C-R2-endo	1.99	2.58	0.59
C'-R2-endo	2.33	2.09	0.24
C-R2-exo	1.99	2.64	0.65
C'-R2-exo	2.43	2.04	0.39
C-R3-endo	2.02	2.50	0.48
C'-R3-endo	2.31	2.13	0.18
C-R3-exo	1.97	2.79	0.82
C'-R3-exo	2.52	2.03	0.49
C-R4	2.34	2.20	0.14

Table 11. Distances of forming C–C σ-bonds for reactions involving C and Un alkenes (M06-2X/6-31+G(d,p)).

Transition State	Ca-Cb (Å)	Cc-Cd (Å)	Difference Between Ca-Cb and Cc-Cd (Å)
C-U1-endo	2.13	2.28	0.15
C-U1-exo	2.03	2.37	0.34
C-U2-endo	2.18	2.27	0.09
C'U2-endo	2.20	2.24	0.04
C-U2-exo	1.94	2.53	0.59
C'-U2-exo	2.08	2.28	0.20
C-U3-endo	2.28	2.12	0.16
C'-U3-endo	2.03	2.43	0.40
C-U3-exo	1.91	2.72	0.81
C'-U3-exo	2.49	2.00	0.49
C-U4-endo	2.10	2.31	0.21
C'-U4-endo	2.11	2.26	0.15
C-U4-exo	2.10	2.31	0.21
C'-U4-exo	2.17	2.24	0.07

Table 12. Distances of forming C–C σ-bonds for reactions involving A (M06-2X/6-31+G(d,p)).

Transition State	Ca-Cb (Å)	Cc-Cd (Å)	Difference Between Ca-Cb and Cc-Cd (Å)	Transition State	Ca-Cb (Å)	Cc-Cd (Å)	Difference Between Ca-Cb and Cc-Cd (Å)
A-R1-endo	2.37	2.39	0.02	**A-U1-endo**	2.31	2.39	0.08
A-R1-exo	2.31	2.45	0.14	**A-U1-exo**	2.30	2.43	0.13
A-R2-endo	2.25	2.48	0.23	**A-U2-endo**	2.34	2.36	0.02
A'-R2-endo	2.41	2.34	0.07	**A'-U2-endo**	2.33	2.38	0.05
A-R2-exo	2.24	2.52	0.28	**A-U2-exo**	2.19	2.53	0.34
A'-R2-exo	2.42	2.33	0.09	**A'-U2-exo**	2.36	2.33	0.03
A-R3-endo	2.23	2.50	0.27	**A-U3-endo**	2.24	2.38	0.14
A'-R3-endo	2.40	2.31	0.09	**A'-U3-endo**	2.34	2.36	0.02
A-R3-exo	2.16	2.77	0.61	**A-U3-exo**	2.09	2.66	0.57
A'-R3-exo	2.51	2.24	0.27	**A'-U3-exo**	2.46	2.24	0.22
A-R4	2.43	2.29	0.14	**A-U4-endo**	2.30	2.31	0.01
				A'-U4-endo	2.19	2.42	0.23
				A-U4-exo	2.24	2.44	0.20
				A'-U4-exo	2.36	2.33	0.03

Table 13. Distances of forming C–C σ-bonds for reactions 1-3 (M06-2X/6-31+G(d,p)).

Transition State	Ca-Cb (Å)	Cc-Cd (Å)	Difference Between Ca-Cb and Cc-Cd (Å)
1-2-endo	2.05	2.45	0.4
1'-2-endo	2.41	2.10	0.31
1-2-exo	2.03	2.42	0.39
1'-2-exo	2.32	2.10	0.22
3	2.11	2.41	0.30
4-5-endo	2.08	2.44	0.36
4'-5-endo	2.22	2.25	0.03
4-5-exo	2.10	2.39	0.29
4'-5-exo	2.17	2.27	0.10

Aromaticity. As mentioned above, decreased aromaticity of cycloaddition partners has been associated with increased reactivity for related systems, i.e., such molecules have less to lose upon cycloaddition. To explore that possibility for the zwitterions examined here, we computed NICS values for **A-C** (in the plane of their rings, NICS(0), and 1 Å above those planes, NICS(1); Table 14).[21] NICS values should be more negative for systems with stronger cyclic delocalization (here, reflected in ring current and associated with the immeasurable quantity of aromaticity). Our computed NICS values for zwitterion reactants are negative but close to zero and do not track with predicted activation barriers for cycloaddition, again emphasizing that making reactant-based reactivity arguments for these systems is dangerous. NICS values for TSSs also do not track with computed barriers (see Supporting Information for details). However, loose correlations between differences in NICS values for reactants and TSSs are observed (e.g., Figure 5; see SI for others), indicating that losses to aromaticity upon

cycloaddition do play a role.

Table 14. NICS(0) and NICS(1) values calculated at the M06-2X/6-31+G(d,p) level of theory for A, B and C

molecule	NICS(0)	NICS(1)
A	-1.5	-5.5
B	-2.9	-5.5
C	-0.4	-4.4

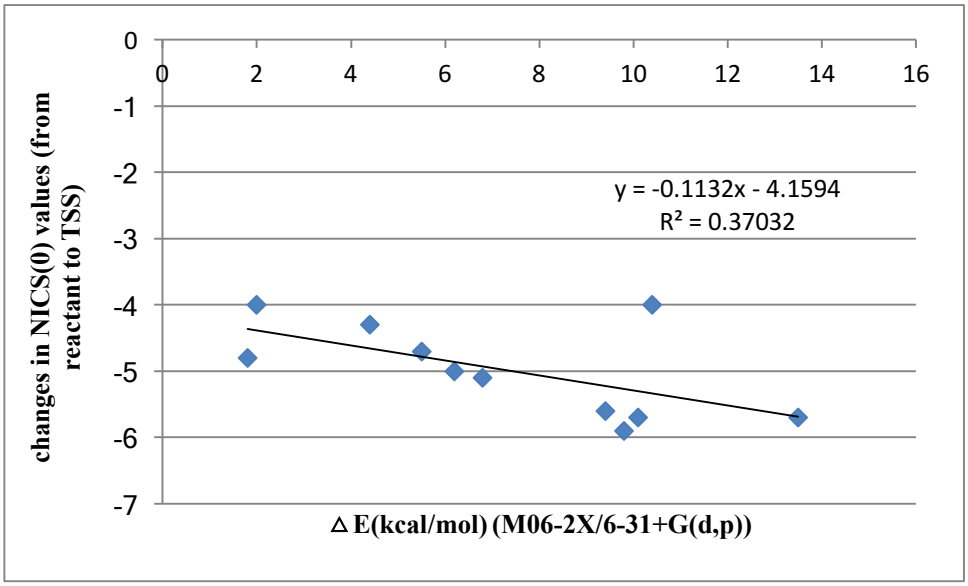

Figure 5. Changes in NICS(0) values (from reactant to TSS) vs. activation barriers (ΔE) of Table 1 reactions (see Supporting Information for plots for other reactions).

Distortion-Interaction Analysis. Distortion-interaction/activation strain analyses were applied to all reactions.[32] Which of total (alkene + zwitterion) distortion energies and individual distortion energies correlates best with predicted barriers varies (Figure 6-8; see Supporting Information for additional information), but, in general, total distortion energies for **B** and **C** (Table 1-4 reactions) are higher than those for **A** (Table 5 reactions) and this appears to be a result of increased distortion in zwitterions upon O→N substitution. For some systems, interaction energies display reasonably strong

correlations (Figure 9), and, in general, interaction energies are lower for **A** than for **B** and **C**. As such, the decreased reactivity for **B** and **C** compared to **A** is more consistent with a distortion effect (which would include aromaticity reduction) than an interaction effect (which would include HOMO-LUMO interactions).

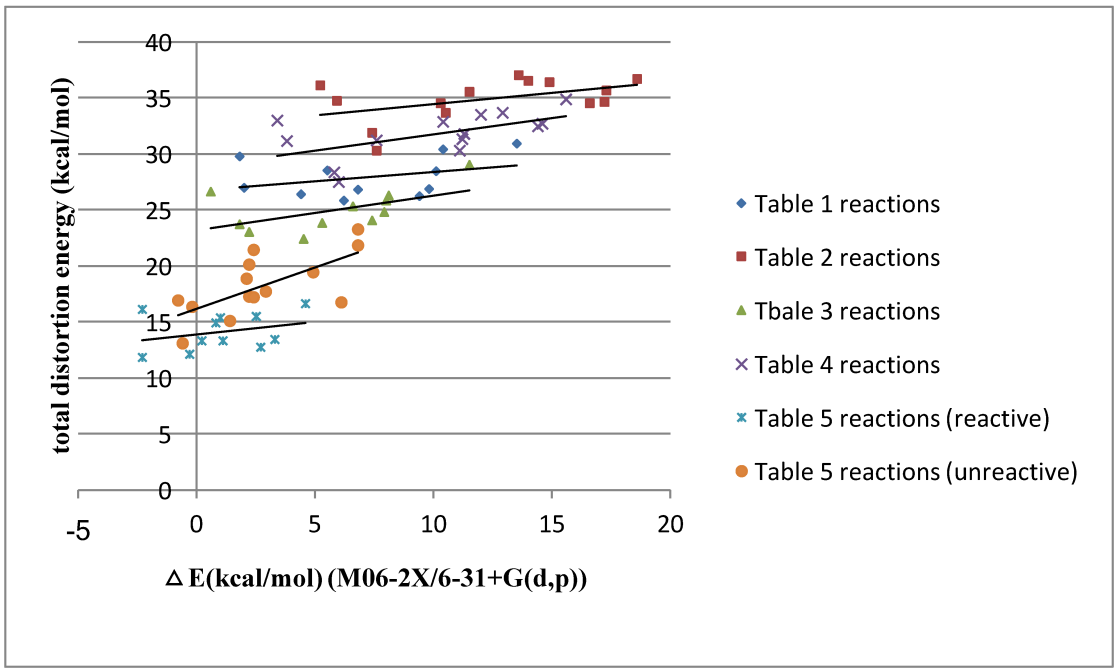

Figure 6. Total distortion energies vs. activation barriers (ΔE) of Table 1-6 reactions (Table 1 reactions: y = 0.1643x + 26.714, R^2 = 0.1165; Table 2 reactions: y = 0.2001x + 32.409, R^2 = 0.2231; Table 3 reactions: y = 0.3117x + 23.161, R^2 = 0.2914; Table 4 reactions: y = 0.2884x + 28.841, R^2 = 0.3287; Table 5 reactions (reactive): y = 0.2305x + 13.85, R^2 = 0.0925; Table 5 reactions (unreactive): y = 0.742x + 16.159, R^2 = 0.4632)

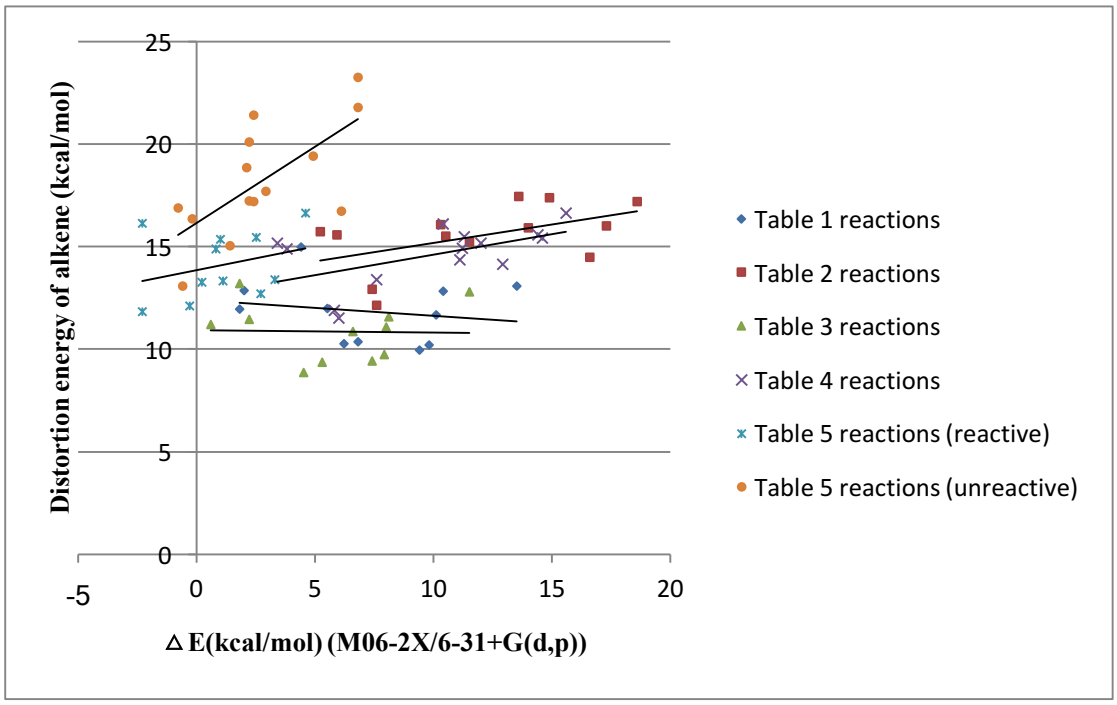

Figure 7. Distortion energies of alkene vs. activation barriers (ΔE) of Table 1-6 reactions (Table 1 reactions: y = -0.0768x + 12.382, R^2 = 0.0336; Table 2 reactions: y = 0.1797x + 13.378, R^2 = 0.254; Table 3 reactions: y = -0.0128x + 10.936, R^2 = 0.0009; Table 4 reactions: y = 0.2002x + 12.607, R^2 = 0.3016 ; Table 5 reactions (reactive): y = 0.2305x + 13.85, R^2 = 0.0925; Table 5 reactions (unreactive): y = 0.742x + 16.159, R^2 = 0.4632)

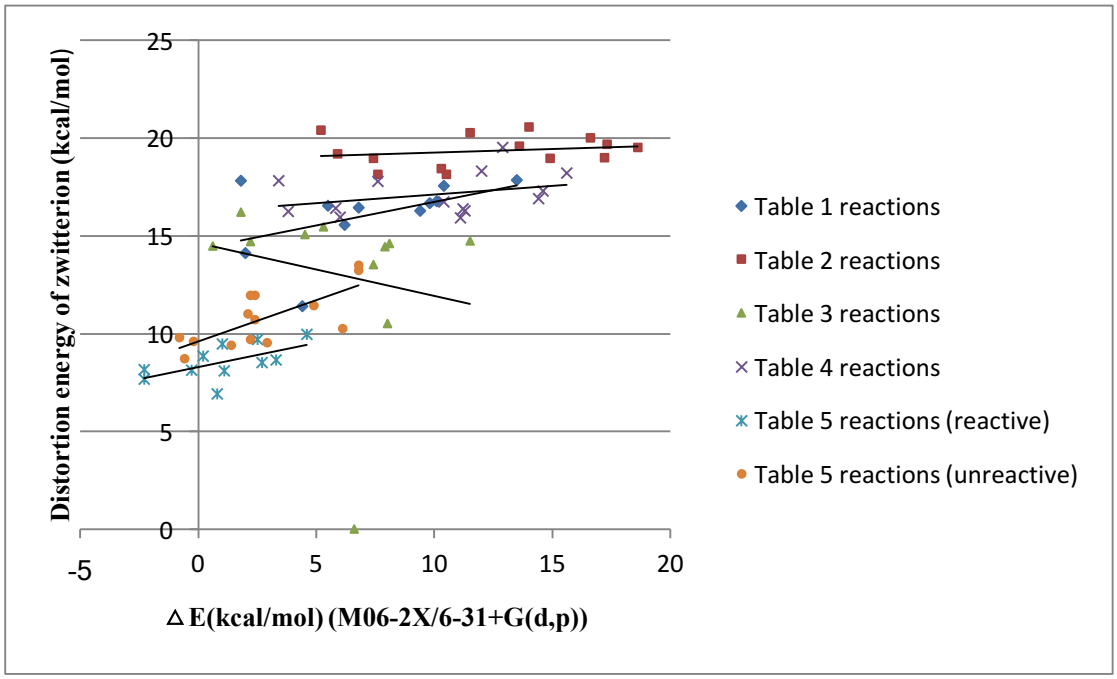

Figure 8. Distortion energies of zwitterion vs. activation barriers (ΔE) of Table 1-6 reactions (Table 1 reactions: y = 0.2411x + 14.332, R^2 = 0.2265; Table 2 reactions: y = 0.0366x + 18.894, R^2 = 0.0427; Table 3 reactions: y = -0.2694x + 14.624, R^2 = 0.0376; Table 4 reactions: y = 0.0882x + 16.233, R^2 = 0.1108; Table 5 reactions (reactive): y = 0.2463x + 8.3009, R^2 = 0.3511; Table 5 reactions (unreactive): y = 0.4227x + 9.6038, R^2 = 0.5348)

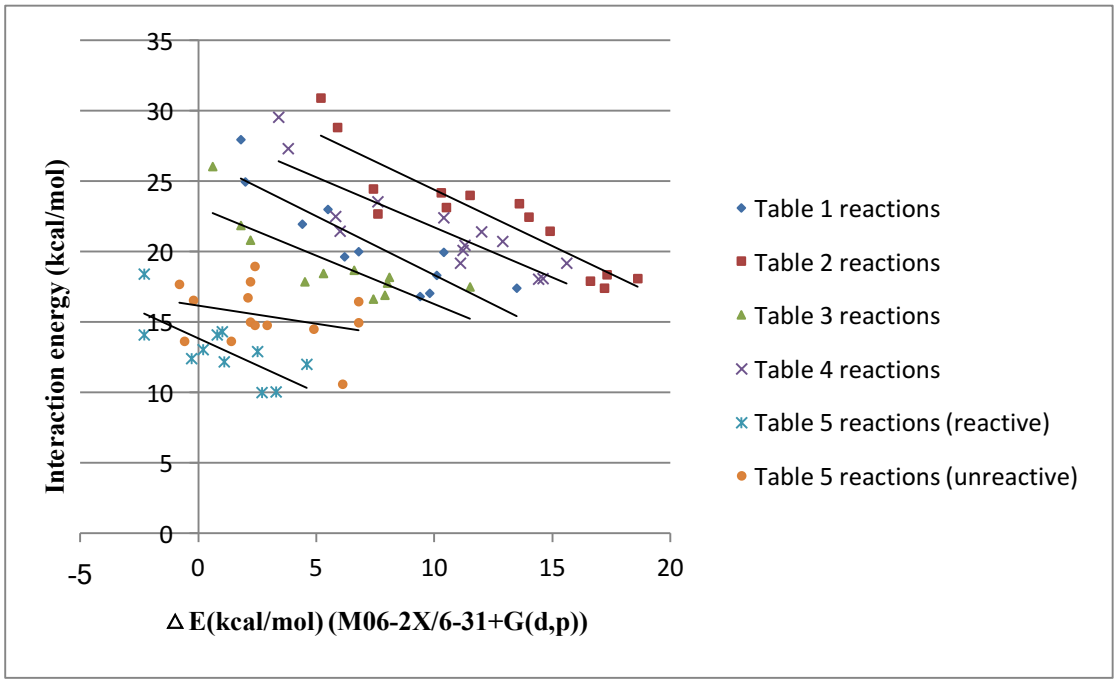

Figure 9. Interaction energies vs. activation barriers (ΔE) of Table 1-6 reactions (Table 1 reactions: y = -0.8357x + 26.714, R^2 = 0.7732; Table 2 reactions: y = -0.7999x + 32.409, R^2 = 0.8211; Table 3 reactions: y = -0.6883x + 23.161, R^2 = 0.6672; Table 4 reactions: y = -0.7116x + 28.841, R^2 = 0.7487; Table 5 reactions (reactive): y = -0.258x + 16.159, R^2 = 0.0945; Table 5 reactions (unreactive): y = -0.258x + 16.159, R^2 = 0.0945)

Synthetic Relevance. *Barriers:* For all the synthetically relevant reactions shown in Figure 1, our predicted barriers are low enough to be consistent with the experimental reaction temperatures. *Selectivity for reaction (1):* The reported product for reaction (1) is the 1-2-exo product (Figure 1).[4] Depending on the level of theory used, either this product or the 1'-2-endo product (the regioisomer) is predicted to have the lowest energy TSS, but these two TSSs are always predicted to be close in energy (Table 6). No 1'-2-endo was observed in the experiment. The yield of 1-2-exo product was 54%, and the yield of 1-2-endo was 36%. Our methods here are not able to capture the product distribution, besides predicting that the 1-2-exo product should be a major product. *Selectivity for reaction (2):* For reaction (2), only the TSS leading to the observed product was computed, since this system is geometrically constrained. *Selectivity for*

reaction (3): For reaction (3), we predict preferential formation of the 4-5-endo product (Table 6), but the 4-5-exo product was reported to predominate (90% yield).[5] Here we predict the correct regioselectivity but not the correct diastereoselectivity. *Selectivity for reaction (4):* For reaction (4), a 2:1 ratio of 6-7 to 6'-7 was reported,[7] and we predict that 6-7 will predominate. In this case, our prediction matches experiment. *Overall:* In general, regioselectivity is readily predicted with standard DFT methods for these systems, but endo/exo selectivity predictions are not reliable. A similar situation has been observed for Diels-Alder reactions.[33] While this situation could improve if ostensibly better levels of theory are employed, that is not guaranteed, since, for example, different reactions were run under different conditions by different chemists, selectivities are often not high ($\Delta\Delta G^{\ddagger} < 2$ kcal/mol), and non-statistical dynamic effects may play important roles.[11] Still, our results should be internally consistent and we have no reason to doubt the validity of the observed *trends*.

Conclusions

A range of (5+2) cycloadditions involving oxidopyridinium zwitterions were modeled using several DFT methods and compared to analogous reactions involving oxidopyrilium zwitterions. From the results of these computations, a general picture of oxidopyridinium cycloaddition chemistry arises. Oxidopyridinium zwitterions are predicted to be less reactive than oxidopyrilium ions. This reduced reactivity is best correlated not to the relative energies of frontier orbitals or interactions involving them, but rather to energetic penalties for zwitterion distortion, which is related in part to changes in aromaticity upon cycloaddition.

ASSOCIATED CONTENT

The Supporting Information containing additional analyses and computed coordinates and energies is available free of charge via the Internet at http://pubs.acs.org

AUTHOR INFORMATION

Corresponding Author

*E-mail: djtantillo@ucdavis.edu

ORCID

Dean J. Tantillo: 0000-0002-2992-8844

Notes

The authors declare no competing financial interest.

ACKNOWLEDGMENTS

We gratefully acknowledge support from the National Science Foundation (CHE-1856416 and supercomputing resources through a grant from the XSEDE program: CHE-030089).

References

1. An oxidopyrylium-alkene cycloaddition has also been suggested as part of a possible biosynthetic route to the polygalolides; see: Nakamura, S.; Sugano, Y.; Kikuchi, F.; Hashimoto Total synthesis and absolute stereochemistry of polygalolides A and BS. *Angew. Chem., Int. Ed.* **2006**, *45*, 6532-6535.
2. Seminal reports: (a) Hendrickson, J. B.; Farina, J. S. A new 7-ring cycloaddition reaction. *J. Org. Chem.* **1980**, *45*, 3359-3361. (b) Hendrickson, J. B.; Farina, J. S. A simple synthesis of 8-and 10-membered carbocyclic rings. *J. Org. Chem.* **1980**, *45*, 3361-3363. (c) Sammes, P. G.; Street, L. J. Stereoselective synthesis of the "cyathin" diterpene skeleton via an intramolecular pyrylium ylide-alkene cyclization. *J. Chem. Soc., Chem. Commun.* **1982**, 1056-1057.
3. Selected examples of oxidopyrylium-alkene cycloadditions in natural products synthesis: (a) Sammes, P. G.; Street, L. J. Stereoselective synthesis of the "cyathin" diterpene skeleton via an intramolecular pyrylium ylide-alkene cyclization. *J. Chem. Soc.*, *Chem. Commun.* **1983**, 666-668. (b) Wender, P. A.; Lee, H. Y.; Wilhelm, R. S.; Williams, P. D. Studies on tumor promoters. 7. The synthesis of a potentially general precursor of the tiglianes, daphnanes, and ingenanes. *J. Am. Chem. Soc.* **1989**, *111*, 8954-8957. (c) Bauta, W.; Booth, J.; Bos, M. E.; DeLuca, M.; Dioazio, L.; Donohoe, T.; Magnus, N.; Magnus, P.; Mendoza, J.; Pye, P.; Tarrant, J.; Thom, S.; Ujjainwalla F. New strategy for the synthesis of the taxane diterpenes: Formation of the BC-rings of taxol via a [5+ 2]-pyrylium ylide-alkene cyclization, ring expansion strategy. *Tetrahedron Lett.* **1995**, *36*, 5327-5330. (d) Marshall, K. A.; Mapp, A. K.; Heathcock, C. H. Synthesis of a 2, 7-Dioxatricyclo [4.2. 1.03, 8] nonane: A Model

Study for Possible Application in a Synthesis of Dictyoxetane. *J. Org. Chem.* **1996**, *61*, 9135-9145. (e) Magnus, P.; Diorazio, L.; Donohoe, T. J.; Giles, M.; Pye, P.; Tarrant, J.; Thom, S. Taxane diterpenes 3: Formation of the eight-membered B-ring by semi-pinacol rearrangement. *Tetrahedron* **1996**, *52*, 14147-14176. (f) Wender, P. A.; Rice, K. D.; Schnute, M. E. The first formal asymmetric synthesis of phorbol. *J. Am. Chem. Soc.* **1997**, *119*, 7897- 7898. (g) Baldwin, J. E.; Mayweg, A. v. W.; Pritchard, G. J.; Adlington, R. M. Expedient synthesis of a highly substituted tropolone via a 3-oxidopyrylium [5+ 2] cycloaddition reaction. *Tetrahedron Lett.* **2003**, *44*, 4543-4545. (h) Krishna, U. M.; Srikanth, G. S. C.; Trivedi, G. K.; Kodand, D. D. Asymmetric oxidopyrylium-alkene [5+ 2] cycloaddition: Synthesis of enantiopure oxa-bridged bicyclo [5.4. 0] undecanes. *Synlett* **2003**, *15*, 2383-2385. (i) Snider, B. B.; Grabowski, J. F. Synthesis of (±)-cartorimine. *Tetrahedron Lett.* **2005**, *46*, 823-825. (j) Snider, B. B.; Wu, X.; Nakamura, S.; Hashimoto, S. A Short, Formal, Biomimetic Synthesis of (±)-Polygalolides A and B. *Org. Lett.* **2007**, *9*, 873-874. (k) Katritzky A.R.; Dennis, N. Cycloaddition reactions of heteroaromatic six-membered rings. *Chem. Rev.* **1989**, *89*(4), 827-861. (l) Lu, Y.; Dey, P.N.; Beaudry, C. Intramolecular Pyridinium Oxide Cycloadditions: Systematic Study of Substitution, Diastereoselectivity, and Regioselectivity. *Chem. Eur. J.* **2021**, *27*, 1-6.

4. Jung, M. E.; Zeng, L.; Peng, T.; Zeng, H.; Le, Y.; Su, J. Total synthesis of Bao Gong Teng A, a natural antiglaucoma compound. *J. Org. Chem.* **1992**, *57*, 3528-3530.
5. Ashley, E. R.; Cruz, E. G.; Stoltz, B. M. The total synthesis of (−)-lemonomycin. *J. Am. Chem. Soc.* **2003**, *125*, 15000– 15001.
6. Peese, K. M.; Gin, D. Y. Efficient synthetic access to the hetisine C20-diterpenoid alkaloids. A concise synthesis of nominine via oxidoisoquinolinium-1, 3-dipolar and dienamine-Diels− Alder cycloadditions. *J. Am. Chem. Soc.* **2006**, *128*, 8734–8735.
7. Krüger, S; Gaich, T. Enantioselective, Protecting- Group- Free Total Synthesis of Sarpagine Alkaloids—A Generalized Approach. *Angew. Chem. Int. Ed.* **2015**, *54*, 315–317; Enantioselektive schutzgruppenfreie Totalsynthese von Sarpagin-Alkaloiden–ein generalisierter Zugang. *Angew. Chem.* **2015**, *127*, 320–322.
8. Yang, Y. F.; Liang, Y.; Liu, F.; Houk, K. N. Diels–Alder reactivities of benzene, pyridine, and di-, tri-, and tetrazines: The roles of geometrical distortions and orbital interactions. *J. Am. Chem. Soc.* **2016**, *138*, 1660-1667.
9. (a) Bejcek, L.P.Murelli, R.P. Oxidopyrylium [5+2] cycloaddition chemistry: Historical Perspective and recent advances (2008–2018). *Tetrahedron* **2016**, *74*(21), 2501-2521. (b) Śliwa, W. Cycloaddition reactions of pyridinium ylides and oxidopyridiniums. *Heterocycles* **1996**, *9*, 2005-2029.
10. Singh, V. Krishna, U.M.; Trivedi, G.K. Cycloaddition of oxidopyrylium species in organic synthesis. *Tetrahedron* **2008**, *16*, 3405-3428.
11. Differences in dynamic behavior, including the possibility that post-transition state bifurcations can be involved, have also been discussed: Burns, J. M.; Boittier, E. D. Pathway Bifurcation in the (4 + 3)/(5 + 2)-Cycloaddition of Butadiene and Oxidopyrilium Ylides: The Significance of Molecular Orbital Isosymmetry, *J. Org.*

Chem. **2019**, *84*, 5997-6005.
12. Talbot, A.; Devarajan, D.; Gustafson, S.J.; Fernández, I.; Bickelhaupt, F.M.; Ess, D.H. Activation-Strain Analysis Reveals Unexpected Origin of Fast Reactivity in Heteroaromatic Azadiene Inverse-Electron-Demand Diels–Alder Cycloadditions. *J. Org. Chem.* **2015**, *80,* 548-558.
13. Kamber, D. N.; Liang, Y.; Blizzard, R. J.; Liu, F.; Mehl, R. A.; Houk, K. N.; Prescher, J. A. 1, 2, 4-triazines are versatile bioorthogonal reagents. *J. Am. Chem. Soc.* **2015**, *137*, 8388-8391.
14. Balcar, J.; Chrisam, G.; Huber, F. X.; Sauer, J. Reaktivität von stickstoff-heterocyclen genenüber cyclooctin als dienophil. *Tetrahedron Lett.* **1983**, *24*, 1481-1484.
15. Wang, S. C.; Tantillo D. J. Theoretical studies on synthetic and biosynthetic oxidopyrylium− alkene cycloadditions: pericyclic pathways to intricarene. *J. Org. Chem.* **2008**, *73*, 1516-1523.
16. (a) Schleyer, P. v. R.; Maerker, C.; Dransfeld, A.; Jiao, H.; Hommes, N. J. R. v. E. Nucleus-Independent Chemical Shifts: A Simple and Efficient Aromaticity Probe. *J. Am. Chem. Soc.* **1996**, *118*, 6317-6318.
17. Frisch, M. J.; Trucks, G. W.; Schlegel, H. B.; Scuseria, G. E.; Robb, M. A.; Cheeseman, J. R.; Scalmani, G.; Barone, V.; Mennucci, B.; Petersson, G. A.; Nakatsuji, H.; Caricato, M.; Li, X.; Hratchian, H. P.; Izmaylov, A. F.; Bloino, J.; Zheng, G.; Sonnenberg, J. L.; Hada, M.; Ehara, M.; Toyota, K.; Fukuda, R.; Hasegawa, J.; Ishida, M.; Nakajima, T.; Honda, Y.; Kitao, O.; Nakai, H.; Vreven, T.; Montgomery, J. A., Jr.; Peralta, J. E.; Ogliaro, F.; Bearpark, M.; Heyd, J. J.; Brothers, E.; Kudin, K. N.; Staroverov, V. N.; Keith, T.; Kobayashi, R.; Normand, J.; Raghavachari, K.; Rendell, A.; Burant, J. C.; Iyengar, S. S.; Tomasi, J.; Cossi, M.; Rega, N.; Millam, J. M.; Klene, M.; Knox, J. E.; Cross, J. B.; Bakken, V.; Adamo, C.; Jaramillo, J.; Gomperts, R.; Stratmann, R. E.; Yazyev, O.; Austin, A. J.; Cammi, R.; Pomelli, C.; Ochterski, J. W.; Martin, R. L.; Morokuma, K.; Zakrzewski, V. G.; Voth, G. A.; Salvador, P.; Dannenberg, J. J.; Dapprich, S.; Daniels, A. D.; Farkas, O.; Foresman, J. B.; Ortiz, J. V.; Cioslowski, J.; Fox, D. J.; Gaussian 09, revision D.01; Gaussian Inc.: Wallingford, CT, **2013**.
18. (a) Becke, A.D. A new mixing of Hartree-Fock and local-density-functional theories. *J. Chem. Phys.* **1993**, *98*, 1372-1377. (b) Becke, A.D. Density-functional thermochemistry. III. The role of exact exchange. *J. Chem. Phys.* **1993**, *98*, 5648-5652. (c) Lee, C.; Yang, W.; Parr, R.G. Development of the Colle-Salvetti correlation-energy formula into a functional of the electron density. *Phys. Rev. B* **1988**, *37*, 785-789. (d) Stephens, P.J.; Devlin, F. J.; Chabalowski, C.F.; Frisch, M. J. Ab Initio Calculation of Vibrational Absorption and Circular Dichroism Spectra Using Density Functional Force Fields. *J. Phys. Chem.* **1994**, *98*, 11623-11627. (e) TiradoRives, J.; Jorgensen, W. L. Performance of B3LYP Density Functional Methods for a Large Set of Organic Molecules. *J. Chem. Theory Comput.* **2008**, *4*, 297-306.
19. Grimme, S.; Antony, J.; Ehrlich, S.; Krieg, H. A consistent and accurate ab initio parametrization of density functional dispersion correction (DFT-D) for the 94

elements H-Pu. *J. Chem. Phys.* **2010**, *132*, 154104
20. (a) Zhao, Y.; Truhlar, D. G. Construction of a generalized gradient approximation by restoring the density-gradient expansion and enforcing a tight Lieb–Oxford bound. *Theor. Chem. Acc.* **2008**, *120*, 215. (b) Zhao, Y.; Truhlar, D. G. Density functionals with broad applicability in chemistry. *Acc. Chem. Res.* **2008**, *41*, 157
21. (a) Gonzalez, C.; Schlegel, H. B. Reaction path following in mass-weighted internal coordinates. *J. Phys. Chem.* **1990**, *94*, 5523- 5527. (b) Fukui, K. The path of chemical reactions-the IRC approach. *Acc. Chem. Res.* **1981**, *14*, 363-368
22. Kozuch, S.; Gruzman, D.; Martin, J. M. DSD-BLYP: A general purpose double hybrid density functional including spin component scaling and dispersion correction. *J. Phys. Chem.* **2010**, *114*, 20801-20808.
23. Wheeler, S.E.; Moran, A.; Pieniazek, S. N.; Houk, K.N. Accurate reaction enthalpies and sources of error in DFT thermochemistry for aldol, Mannich, and α-aminoxylation reactions. *J. Phys. Chem.* **2009**, *113*, 10376-10384.
24. Ess, D. H.; Houk, K. N. Activation energies of pericyclic reactions: performance of DFT, MP2, and CBS-QB3 methods for the prediction of activation barriers and reaction energetics of 1, 3-dipolar cycloadditions, and revised activation enthalpies for a standard set of hydrocarbon pericyclic reactions. *J. Phys. Chem.* **2005**, *109*, 9542-9553.
25. Lan, Y.; Zou, L.; Cao, Y. Houk, K. N. Computational methods to calculate accurate activation and reaction energies of 1, 3-dipolar cycloadditions of 24 1, 3-dipoles. *J. Phys. Chem.* **2011**, *115*, 13906-13920.
26. Guner, V.; Khuong, K. S.; Leach, A. G.; Lee, P. S.; Bartberger M. D.; Houk, K. N. A standard set of pericyclic reactions of hydrocarbons for the benchmarking of computational methods: the performance of ab initio, density functional, CASSCF, CASPT2, and CBS-QB3 methods for the prediction of activation barriers, reaction energetics, and transition state geometries. *J. Phys. Chem.* **2003**, *107*, 11445-11459.
27. Wiest, O.; Montiel, D. C.; Houk, K. N. Quantum Mechanical Methods and the Interpretation and Prediction of Pericyclic Reaction Mechanisms. *J. Phys. Chem.* **1997**, *101*, 8378-8388.
28. Wodrich, M. D.; Corminboeuf, C.; Schreiner, P. R.; Fokin, A. A.; Schleyer, P.v.R. Quantum mechanical methods and the interpretation and prediction of pericyclic reaction mechanisms. *Org. Lett.* 2007, *9*, 1851-1854.
29. Wodrich, M. D.; Corminboeuf, C.; Schleyer, P.v.R. Systematic errors in computed alkane energies using B3LYP and other popular DFT functionals. *Org. Lett.* **2006**, *8*, 3631-3634.
30. Matsuda, S. P.; Wilson, W. K.; Xiong, Q. Mechanistic insights into triterpene synthesis from quantum mechanical calculations. Detection of systematic errors in B3LYP cyclization energies. *Org. Biomol. Chem.* **2006**, *4*, 530-543.
31. The Role Of Frontier Orbitals In Chemical Reactions Nobel lecture, 8 December, 1981 by Kenichi Fukui
32. Bickelhaupt, F. M.; Houk, K. N. Analyzing reaction rates with the distortion/interaction- activation strain model. *Ang. Chem. Int. Ed.* **2017**, *56*, 10070-10086.

33. (a) Lording, W.J.; Fallon, T.; Sherburn, M.S.; Paddon-Row, M.N. The simplest Diels–Alder reactions are not endo-selective. *Chem. Sci.*, **2020**, *11*, 11915–11926. (b) McCulley, C. H., PhD Dissertation, University of California, Davis, **2019**.

TOC